



OPEN ACCESS

EDITED BY

Raul Mostoslavsky,
Massachusetts General Hospital Cancer Center,
United States

REVIEWED BY

Yiannis Drosos,
University of Patras, Greece
Alexandre Gaspar Maia,
Mayo Clinic, United States

*CORRESPONDENCE

Sara Patrizi,
✉ sara.patrizi@opbg.net
Evelina Miele,
✉ evelina.miele@opbg.net

[†]These authors have contributed equally to this work and share last authorship

RECEIVED 03 May 2024

ACCEPTED 13 August 2024

PUBLISHED 04 September 2024

CITATION

Patrizi S, Vallese S, Pedace L, Nardini C, Stracuzzi A, Barresi S, Giovannoni I, Abballe L, Antonacci C, Russo I, Di Giannatale A, Alaggio R, Locatelli F, Milano GM and Miele E (2024) Quantification of tumour-infiltrating immune cells through deconvolution of DNA methylation data in Ewing sarcomas. *Front. Epigenet. Epigenom.* 2:1427399. doi: 10.3389/freae.2024.1427399

COPYRIGHT

© 2024 Patrizi, Vallese, Pedace, Nardini, Stracuzzi, Barresi, Giovannoni, Abballe, Antonacci, Russo, Di Giannatale, Alaggio, Locatelli, Milano and Miele. This is an open-access article distributed under the terms of the [Creative Commons Attribution License \(CC BY\)](https://creativecommons.org/licenses/by/4.0/). The use, distribution or reproduction in other forums is permitted, provided the original author(s) and the copyright owner(s) are credited and that the original publication in this journal is cited, in accordance with accepted academic practice. No use, distribution or reproduction is permitted which does not comply with these terms.

Quantification of tumour-infiltrating immune cells through deconvolution of DNA methylation data in Ewing sarcomas

Sara Patrizi^{1*}, Silvia Vallese², Lucia Pedace¹, Claudia Nardini¹, Alessandra Stracuzzi², Sabina Barresi², Isabella Giovannoni², Luana Abballe¹, Celeste Antonacci¹, Ida Russo¹, Angela Di Giannatale¹, Rita Alaggio², Franco Locatelli^{1†}, Giuseppe Maria Milano^{1†} and Evelina Miele^{1*†}

¹Onco-Hematology, Cell Therapy, Gene Therapies and Hemopoietic Transplant, Bambino Gesù Children's Hospital, IRCCS, Rome, Italy, ²Pathology Unit, Bambino Gesù Children's Hospital, IRCCS, Rome, Italy

Ewing Sarcomas (EWS, OMIM#612219) presents a major challenge in pediatric oncology due to its aggressive nature and poor prognosis, particularly in metastatic cases. Genetic fusions involving the *EWSR1* gene and ETS family transcription factors are common in EWS, though other rarer fusions have also been identified. Current standard techniques like immunohistochemistry have failed to fully characterize the immune tumor microenvironment of EWS, hindering insights into tumor development and treatment strategies. Recent efforts apply gene expression datasets to quantify tumor-infiltrating immune cells in EWS. Similar deconvolution techniques can be also applied to DNA methylation (DNAm) arrays, which are much more stable compared to RNA-based methods. This study aims to characterize immune cell infiltration in EWS using DNAm array data. We collected 32 EWS samples from 32 consecutive patients referred to Bambino Gesù Children's Hospital. DNAm analysis was performed by EPIC arrays; data loading, normalization, deconvolution and survival analysis were then performed in R programming environment. We observed a higher content of dendritic cells and longer overall survival in samples with *EWSR1::FLI1* translocation compared to samples with rarer fusions. Moreover, T-memory lymphocytes and monocytes emerged as a significant predictor of overall survival. This study underscores the potential of DNAm arrays in providing robust insights into EWS immune profiles, offering a promising avenue for future research. Further investigations with larger cohorts are warranted to validate these findings and explore additional immune cell types influencing EWS outcomes.

KEYWORDS

Ewing sarcoma, DNA methylation, immune microenvironment, deconvolution, immunotherapy

1 Introduction

Ewing sarcomas (EWS) most often affect the bones and soft tissues in children and young adults and are known for their aggressive nature and their dismal prognosis when diagnosed in the metastatic stage. From a histological perspective, these tumors fall within the category of “undifferentiated small round blue cell sarcomas of bone and soft tissue (WHO 2020 and WHO 2022).” They consist of small, monotonous round cells exhibiting nuclei with finely dispersed chromatin and thin rim of cytoplasm. The cells are arranged in sheets with occasional rosette formation and frequent necrotic areas (Yoshida, 2023; Sbaraglia et al., 2021; Pfister et al., 2022). The differential diagnosis from other Ewing-like sarcomas (ELS), requires molecular characterization (Llobart-Bosch et al., 2009; Italiano et al., 2012; Antonescu, 2014). EWS are characterized by genetic fusions involving an *EWS* gene and an ETS family transcription factor (Delattre et al., 1992). The most frequent fusion involves *EWSR1* (OMIM*133450) and *FLI1* (OMIM*193067), but other rarer rearrangements with the same biological behavior have also been identified (Sorensen and Triche, 1996; Arvand and Denny, 2001).

So far, standard techniques like immunohistochemistry have been unsuccessful in providing a complete characterization of the immune tumour microenvironment of EWS (Paydas et al., 2016; Berghuis et al., 2011). Some efforts have been made using single-cell RNA sequencing (Visser et al., 2023; Cillo et al., 2022), a technique that still presents several challenges and limitations (Robinson et al., 2022). An accurate quantification of tumour-infiltrating immune cells (TIICs), however, would be valuable to shed light on the development and aggressiveness of these tumours and provide new avenues for treatment (Evdokimova et al., 2022).

Recently, Stahl et al. analysed microarray gene expression datasets of primary EWS samples using the CIBERSORT deconvolution algorithm to determine the proportion of 22 immune cell types within bulk tumour tissue (Stahl et al., 2019).

Such deconvolution can be also inferred from DNA methylation (DNAm) arrays, which are more robust than gene expression arrays given the higher stability of DNA compared with RNA (Alberts et al., 2002). Moreover, DNAm data is known to be less influenced by copy number variation than gene expression (Stranger et al., 2007; Houseman et al., 2009), a relevant concern in the field of oncology where most samples display copy number variations. Lastly, DNAm arrays are currently widely used to aid soft tissue sarcoma diagnosis through machine-learning based classifiers (Koelsche et al., 2021), while RNA sequencing currently lacks diagnostic applications. Thus, performing both diagnostic profiling and tumor microenvironment characterization on the same data appears convenient.

The aim of this study is to characterize the relative abundance of immune cells infiltrated in EWS using DNAm array, a technique that is already implemented in the diagnostic workflow of challenging sarcoma cases at our Institution, and to correlate it with patients' survival.

2 Methods

We selected 32 EWS samples from 32 patients with challenging diagnosis referred to our institution and analysed for DNAm profiling (from 2020 to 2024) and, after acquiring informed consent from either

the patient or their legal guardian, retrieved their follow-up information from clinical records (study protocol number 2126_OPBG_2020, reviewed and approved by the Bambino Gesù Children's Hospital Ethical Committee). We reviewed 30/32 cases with available tissue, evaluating parameters that could affect the tumor purity. In detail, we quantified the percentage of inflammatory cells, by CD45 antibody staining (mouse monoclonal antibody, clone 2B11+PD7/26, ready to use, Dako) performed on DAKO OMNIS platform scoring it 0 (<1%), 1 (1–2%), 2 (3–5%), or 3 (>5%); the presence (Yoshida, 2023) or absence (0) of necrosis and collagenized stroma. We calculated a final “total infiltration score” from the sum of the previously described parameters and correlated it with the tumor purity calculated from DNAm deconvolution data.

We extracted both RNA (by ReliaPrep™ FFPE Total RNA kit, Promega) and DNA (by MagPurix FFPE DNA Extraction Kit, Zinexts, Life Science Corporation, New Taipei City, Taiwan) from unstained sections of paraffin blocks containing at least 70% tumour cells.

We used either whole-transcriptome RNA sequencing (in 3/32 cases), RT-PCR or Archer FusionPlex custom panel to detect the presence of gene fusions, as described previously (Patrizi et al., 2024).

We carried out DNA methylation (DNAm) analysis using the Human MethylationEPIC v1.0 and v2.0 BeadChip arrays (Illumina), according to the manufacturer's instructions, as previously reported (Salgado et al., 2023).

We analyzed raw BeadChip data with R package ChAMP (version 2.26.0) (Tian et al., 2017), that was chosen because it conveniently integrates existing analysis tools into a single pipeline. We loaded v1.0 and v2.0 data separately with method “minfi” (Aryee et al., 2014) and filtering out probes with detection *p*-value > 0.01. Then, we merged v1.0 and v2.0 raw beta values according to probe name and genomic position. We normalized the merged raw methylation beta values using the BMIQ method (Teschendorff et al., 2013), confirmed the absence of confounding batch factors with function champ. SVD, and performed immune cell deconvolution through package MethylResolver (Arneson et al., 2020). This deconvolution method can resolve fractions of 11 immune cell types, both in terms of relative abundance to the total amount of immune cells and of absolute abundance scaled according to tumor purity (the percentage of tumor cells in the total tissue), without the need to develop a cancer-specific signature.

We used two-tailed heteroschedastic Student's T-test to evaluate the statistical significance of differences in immune cell content between sample groups, and Kaplan-Meier analysis performed with R package survival (<https://CRAN.R-project.org/package=survival>) to assess the relationship between immune cell content and overall survival. For Kaplan-Meier analysis, we determined the optimal cutpoint for each continuous variable using function surv_cutpoint from package survminer (<https://CRAN.R-project.org/package=survminer>), that uses the maximally selected rank statistics from the maxstat R package to divide a continuous variable in order to obtain the most significant correlation with survival.

3 Results

The study cohort includes 32 tumors with histological diagnosis of Ewing sarcoma from 32 consecutive patients less than 30 years old

TABLE 1 Characteristics of the selected EWS samples, including gender, age at diagnosis, status at last follow up (DOD = Dead of Disease, NA = Not Available), translocation, and translocation type.

Case #	Gender (M/F)	Age at diagnosis (years)	Status at last follow up	Overall survival (years)	Translocation
1	M	5	NA	NA	EWSR1::ETV4
2	F		NA	NA	EWSR1::FLI1
3	F	14	DOD	1.58	EWSR1::FLI1
4	M	16	ALIVE	4.17	EWSR1::FLI1
5	M	12	ALIVE	1.42	EWSR1::FLI1
6	F	5	ALIVE	4.25	EWSR1::FLI1
7	M	11	DOD	3.75	EWSR1::FLI1
8	F	12	DOD	2.08	EWSR1::FLI1
9	F	17	ALIVE	4.92	EWSR1::FLI1
10	F	9	NA	NA	EWSR1::FLI1
11	F	34	NA	NA	EWSR1::FLI1
12	M	10	DOD	0.08	EWSR1::FLI1
13	M	6	DOD	1.08	EWSR1::ERG
14	F	18	DOD	0.58	EWSR1::FLI1
15	M	11	NA	NA	EWSR1::FLI1
16	F	4	NA	NA	EWSR1::FLI1
17	F	9	NA	NA	EWSR1::FLI1
18	F	27	NA	NA	EWSR1::FLI1
19	F	10	DOD	0.58	EWSR1::ERG
20	F	13	ALIVE	1.25	EWSR1::FLI1
21	F	16	ALIVE	1.17	EWSR1::FLI1
22	F	10	ALIVE	1.08	EWSR1::FLI1
23	M	1	ALIVE	0.83	EWSR1::FLI1
24	M	2	ALIVE	0.83	EWSR1::ETV4
25	M	6	ALIVE	0.67	EWSR1::FLI1
26	M	9	ALIVE	0.92	EWSR1::FLI1
27	M	7	ALIVE	0.67	EWSR1::FLI1
28	M	11	DOD	2.58	EWSR1::FLI1
29	M	16	ALIVE	0.42	EWSR1::FLI1
30	F	13	ALIVE	0.25	EWSR1::FLI1
31	M	15	ALIVE	0.50	EWSR1::FLI1
32	F	5	ALIVE	4.83	EWSR1::FLI1

at the time of diagnosis. Patients’ characteristics are summarized in [Table 1](#). The cohort included 17 females (53%) and 15 males (47%). The median age was 11 years old. Most samples (28/32) had the *EWSR1::FLI1* fusion, while 4 had other translocations involving *EWSR1* (2 *EWSR1::ERG*, 2 *EWSR1::ETV4*). In 30/32 cases the tissue was obtained at the moment of diagnosis of the primary tumor. One case was a very late relapse, while for 1 this information was not available ([Supplementary Table S1](#)). The level of immune infiltration

observable through histological review was generally extremely low and did not allow the quantification of specific cell types ([Supplementary Table S1](#); [Supplementary Figure S1](#)). We also evaluated further histological aspects that could influence tumor purity, observing necrosis/haemorrhagy in 15/30 and fibrosis in 13/30 cases. However, we observed no correlation between the total infiltration score and DNAm-inferred tumor purity (correlation score 0.26).

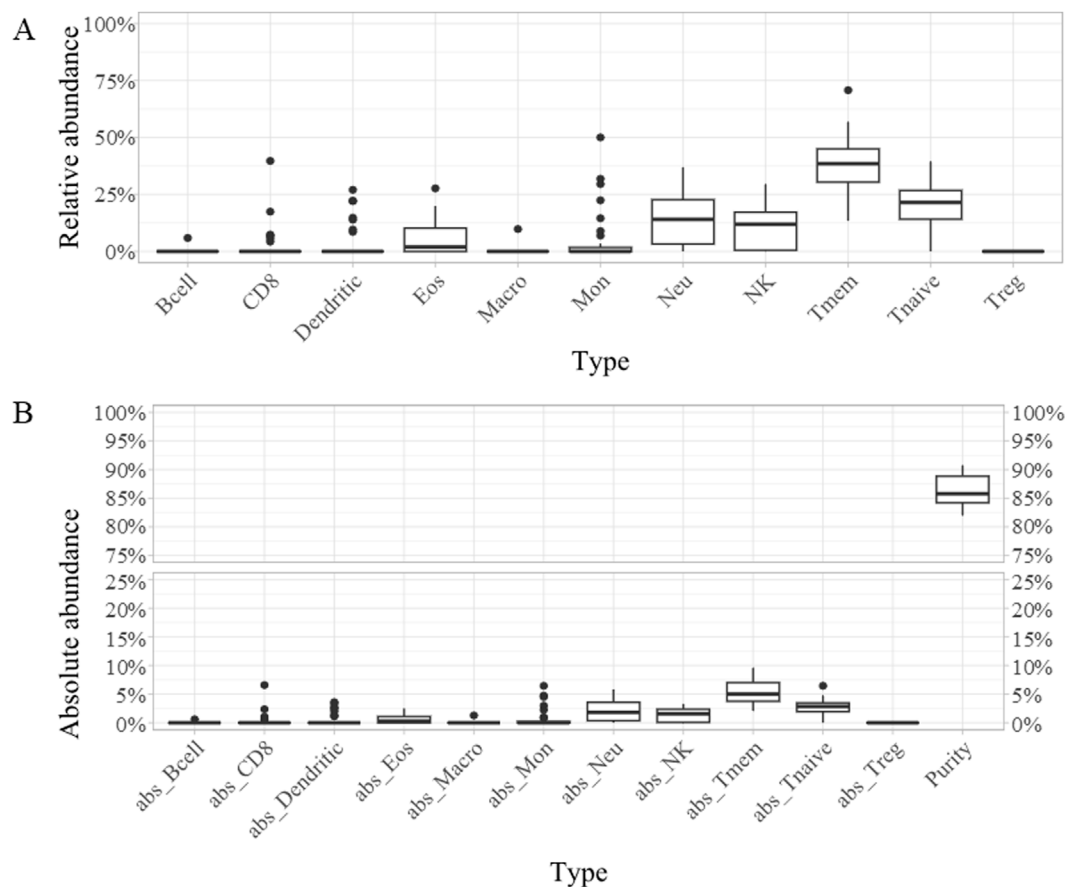


FIGURE 1
 Boxplots representing the relative (A) and absolute [“abs,” (B)] abundance of each of the 11 cell types detected across the whole cohort: B cells (Bcell), CD8 lymphocytes (CD8), dendritic cells (Dendritic), eosinophiles (Eos), macrophages (Macro), monocytes (Mon), neutrophils (Neu), natural killer cells (NK), T-memory lymphocytes (Tmem), T-naive lymphocytes (Tnaive), T-regulatory lymphocytes (Treg), tumor purity (Purity).

The immune cell deconvolution returned the abundance of 11 cell types, both relatively to the total amount of immune cells (relative abundance) and to the total tissue (absolute abundance).

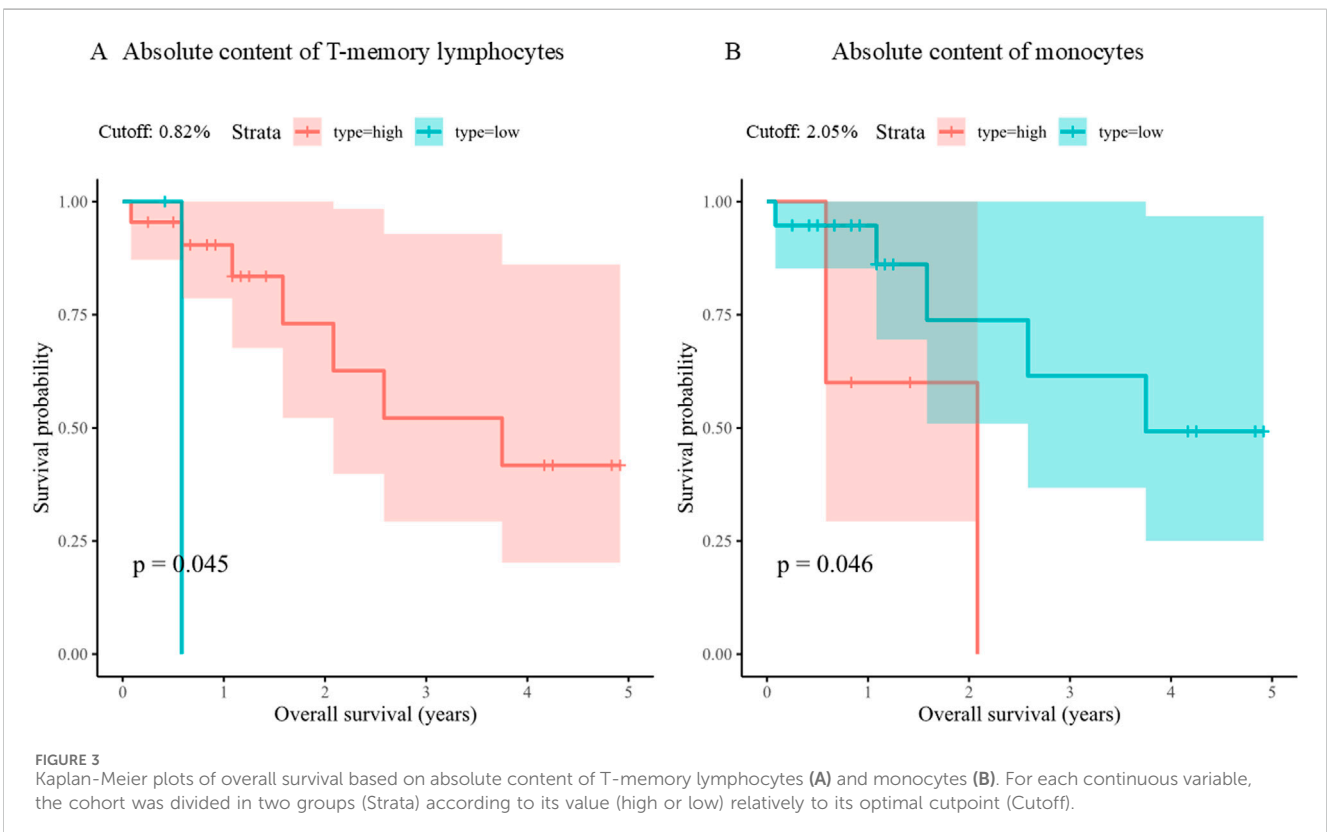
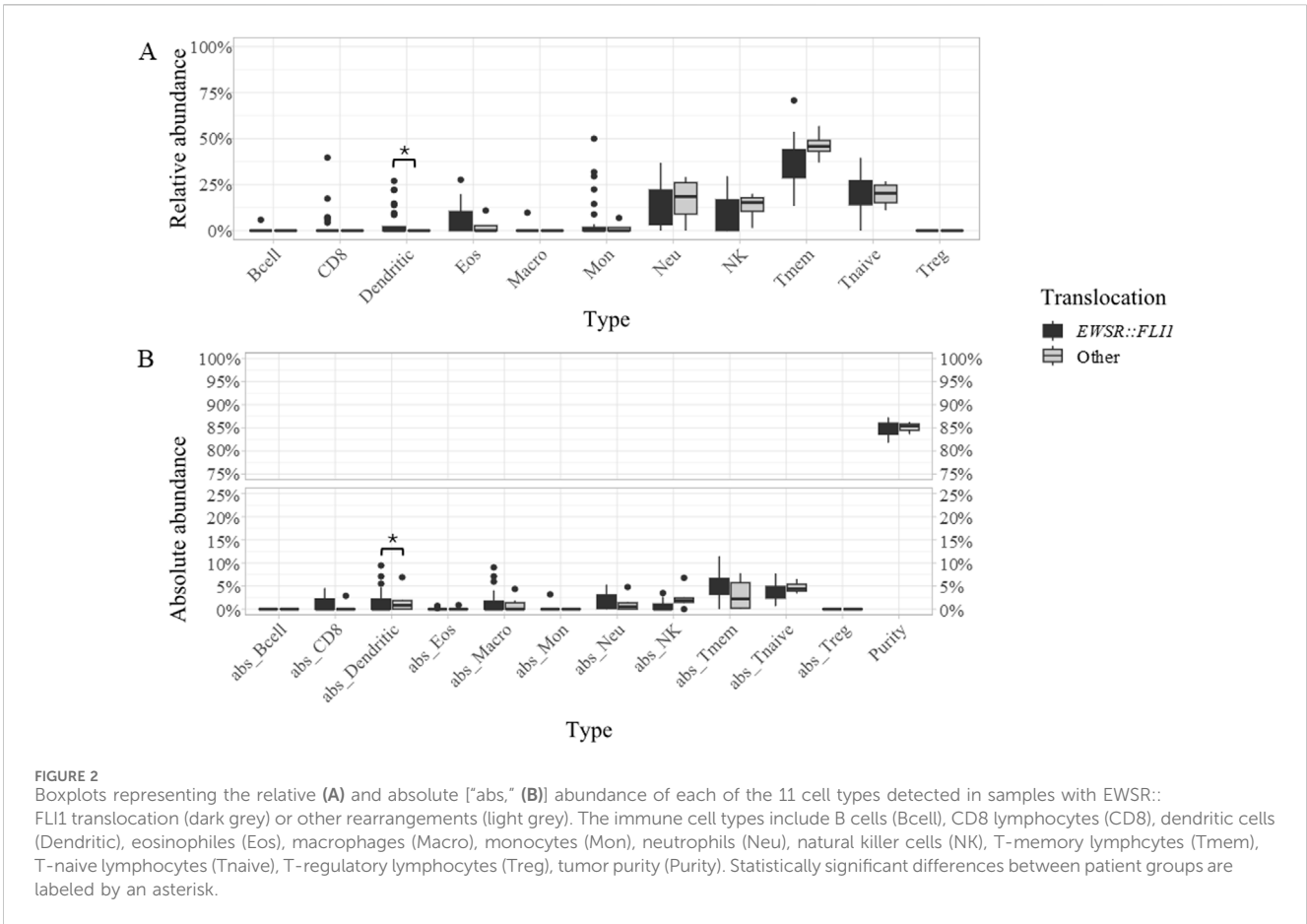
Across the whole cohort, the most abundant cell types were T-memory lymphocytes (“Tmem,” mean percentage 37.49%), T-naïve lymphocytes (mean percentage 20.56%), neutrophils (mean percentage 14.10%), and natural killer (NK) cells (mean percentage 10.44%) (Figures 1A, B; Supplementary Table S1). When compared to *EWSR1::FLI1* rearranged, samples with rarer translocations displayed a significantly lower mean content of dendritic cells, both absolute (0% versus 0.61%) and relative to the immune component (0% versus 4.37%) (Figures 2A, B; Supplementary Table S1).

Follow-up was available for 24/32 patients (Table 1). Samples with *EWSR1::FLI1* translocation showed a significantly longer overall survival than samples with rarer alterations (Supplementary Table S1). Moreover, Kaplan-Meier analysis revealed two variables significantly associated with overall survival in the whole cohort. One was the absolute content of T-memory lymphocytes, that correlated with better outcomes (Bonferroni *p*-value = 0.04) when it was higher than 2.05% (Figure 3A), and the other was the absolute content of monocytes, that was associated with higher overall survival

when lower than 0.82% (Figure 3B; Supplementary Table S2). Moreover, patients with tumor purity lower than 83.73% had a higher survival probability, although not significantly (Bonferroni *p*-value = 0.11) (Supplementary Table S2).

4 Discussion

Our cohort included 32 patients with a median age of 11 years at diagnosis, which reflects the age of peak incidence of Ewing sarcoma. However, we did not observe the same male prevalence that is reported in literature (Durer et al., 2024). The immune cell deconvolution showed that the most abundant cell types across the cohort were lymphocytes, representing 60.63% of all TIICs considering Tmem, T-naive and CD8 lymphocytes (2.54%), followed by neutrophils (mean percentage 14.10%). This result differs from the prevalence of macrophages detected from RNA sequencing data by Stahl et al. Lymphocyte prevalence has been reported as a characteristic of tumours with “hot” immune microenvironment (Wang et al., 2023), whereas Ewing sarcoma is known as a “cold” tumour, with low expression of neoantigens and low leucocyte infiltration (Evdokimova et al., 2022). The low and



homogenous absolute immune cell content measured for each sample in our cohort supports the latter concept.

In our cohort, samples with *EWSR1::FLII* translocation presented significantly longer overall survival and higher dendritic cells content (both relative and absolute) than the cases with different translocations. Since dendritic cells are known to play an important role in presenting tumour antigens to the immune system, and are often downregulated in metastatic and aggressive cancers (Del Prete et al., 2023), these two observations could be correlated. However, functional studies on a larger cohort would be needed to reach a definite conclusion.

We also found a significant correlation of longer overall survival with higher relative Tmem content, which supports previous reports of their important anti-tumor role (Liu et al., 2020). In some contexts, however, the presence of tissue-resident memory T cells has been related to a stronger recruitment of other immune cells, causing a loss of MHC class I protein expression on tumour cells and thus favoring their escape from immune response (Weeden et al., 2023). Therefore, the role of Tmem in the immune microenvironment of EWS appears intriguing and worthy of further investigations. Patients with lower tumor purity (and in consequence with higher immune infiltrate) also had better outcomes, albeit not significantly, which leads us to hypothesize that, even in a cold tumor microenvironment, an immune response can limit the cancerous cell proliferation.

Our study shows that TIICs proportions in EWS can be inferred from DNA methylation data, thus providing an alternative to traditional techniques or gene expression arrays. A weakness of our study is the lack of correlation between DNAm-inferred tumor purity and our total infiltration score derived from histopathological evaluation. We can speculate that this could be due to the selection of a different histological section for DNA methylation and histological review, or to method-specific biases. Further specific studies on larger sample groups are needed, to better assess the correlation between deconvolution results from different data sources and histopathology, and to confirm the cell types we identified as directly or inversely correlated with survival.

Data availability statement

The data presented in the study are deposited in the NCBI GEO repository, accession number GSE276012.

Ethics statement

The studies involving humans were approved by Comitato Etico Ospedale Pediatrico Bambino Gesù. The studies were conducted in accordance with the local legislation and institutional requirements. Written informed consent for participation in this study was provided by the participants' legal guardians/next of kin.

Author contributions

SP: Conceptualization, Writing–original draft, Writing–review and editing, Formal Analysis, Visualization. SV: Data curation,

Resources, Writing–review and editing. LP: Investigation, Writing–review and editing. CN: Investigation, Writing–review and editing. AS: Resources, Data curation, Writing–review and editing. SB: Investigation, Writing–review and editing. IG: Investigation, Writing–review and editing. LA: Investigation, Writing–review and editing. CA: Investigation, Writing–review and editing. IR: Data curation, Resources, Writing–review and editing. AD: Data curation, Resources, Writing–review and editing. RA: Supervision, Writing–review and editing. FL: Supervision, Writing–review and editing. GM: Conceptualization, Data curation, Funding acquisition, Resources, Supervision, Writing–original draft, Writing–review and editing. EM: Conceptualization, Data curation, Funding acquisition, Resources, Supervision, Writing–original draft, Writing–review and editing.

Funding

The author(s) declare that financial support was received for the research, authorship, and/or publication of this article. This research was supported by the Italian Ministry of Health with “Current Research funds” (202005_ONCO_MIELE to EM; and 202203_FBG_MILANO.1.15 to GM).

Acknowledgments

The authors thank Associazione il Cuore grande di Flavio for their support. SP and LA were supported by Fondazione Umberto Veronesi.

Conflict of interest

The authors declare that the research was conducted in the absence of any commercial or financial relationships that could be construed as a potential conflict of interest.

The author(s) declared that they were an editorial board member of *Frontiers*, at the time of submission. This had no impact on the peer review process and the final decision.

Publisher's note

All claims expressed in this article are solely those of the authors and do not necessarily represent those of their affiliated organizations, or those of the publisher, the editors and the reviewers. Any product that may be evaluated in this article, or claim that may be made by its manufacturer, is not guaranteed or endorsed by the publisher.

Supplementary material

The Supplementary Material for this article can be found online at: <https://www.frontiersin.org/articles/10.3389/freae.2024.1427399/full#supplementary-material>

References

- Alberts, B., Bray, D., Lewis, J., Raff, M., and Roberts, K. (2002). *The molecular biology of the cell*. New York: Garland Science.
- Antonescu, C. (2014). Round cell sarcomas beyond Ewing: emerging entities. *Histopathology* 64 (1), 26–37. doi:10.1111/his.12281
- Arneson, D., Yang, X., and Wang, K. (2020). MethylResolver—a method for deconvoluting bulk DNA methylation profiles into known and unknown cell contents. *Commun. Biol.* 3 (1), 422–513. doi:10.1038/s42003-020-01146-2
- Arvand, A., and Denny, C. T. (2001). Biology of EWS/ETS fusions in Ewing's family tumors. *Oncogene* 20 (40), 5747–5754. doi:10.1038/sj.onc.1204598
- Aryee, M. J., Jaffe, A. E., Corrada-Bravo, H., Ladd-Acosta, C., Feinberg, A. P., Hansen, K. D., et al. (2011). Minfi: a flexible and comprehensive Bioconductor package for the analysis of Infinium DNA methylation microarrays. *Bioinformatics* 30 (10), 1363–1369. doi:10.1093/bioinformatics/btu049
- Berghuis, D., Santos, S. J., Baelde, H. J., Taminiau, A. H., Maarten Egeler, R., Schilham, M. W., et al. (2011). Pro-inflammatory chemokine-chemokine receptor interactions within the Ewing sarcoma microenvironment determine CD8(+) T-lymphocyte infiltration and affect tumour progression. *J. Pathology* 223 (3), 347–357. doi:10.1002/path.2819
- Cillo, A. R., Mukherjee, E., Bailey, N. G., Onkar, S., Daley, J., Salgado, C., et al. (2022). Ewing sarcoma and osteosarcoma have distinct immune signatures and intercellular communication networks. *Clin. Cancer Res.* 28 (22), 4968–4982. doi:10.1158/1078-0432.ccr-22-1471
- Delattre, O., Zucman, J., Plougastel, B., Desmaze, C., Melot, T., Peter, M., et al. (1992). Gene fusion with an ETS DNA-binding domain caused by chromosome translocation in human tumours. *Nature* 359 (6391), 162–165. doi:10.1038/359162a0
- Del Prete, A., Salvi, V., Soriani, A., Laffranchi, M., Sozio, F., Bosisio, D., et al. (2023). Dendritic cell subsets in cancer immunity and tumor antigen sensing. *Cell Mol. Immunol.* 20 (5), 432–447. doi:10.1038/s41423-023-00990-6
- Durer, S., Gasalberti, D. P., and Shaikh, H. (2024). "Ewing sarcoma," in *StatPearls* (Treasure Island (FL): StatPearls Publishing). Available at: <http://www.ncbi.nlm.nih.gov/books/NBK559183/>.
- Evdokimova, V., Gassmann, H., Radvanyi, L., and Burdach, S. E. G. (2022). Current state of immunotherapy and mechanisms of immune evasion in ewing sarcoma and osteosarcoma. *Cancers* 15 (1), 272. doi:10.3390/cancers15010272
- Houseman, E. A., Christensen, B. C., Karagas, M. R., Wrensch, M. R., Nelson, H. H., Wiemels, J. L., et al. (2009). Copy number variation has little impact on bead-array-based measures of DNA methylation. *Bioinformatics* 25 (16), 1999–2005. doi:10.1093/bioinformatics/btp364
- Italiano, A., Sung, Y. S., Zhang, L., Singer, S., Maki, R. G., Coindre, J. M., et al. (2012). High prevalence of CIC fusion with double-homeobox (DUX4) transcription factors in EWSR1-negative undifferentiated small blue round cell sarcomas. *Genes, Chromosomes Cancer* 51 (3), 207–218. doi:10.1002/gcc.20945
- Koelsche, C., Schrimpf, D., Stichel, D., Sill, M., Sahm, F., Reuss, D. E., et al. (2021). Sarcoma classification by DNA methylation profiling. *Nat. Commun.* 12, 498. doi:10.1038/s41467-020-20603-4
- Liu, Q., Sun, Z., and Chen, L. (2020). Memory T cells: strategies for optimizing tumor immunotherapy. *Protein Cell* 11 (8), 549–564. doi:10.1007/s13238-020-00707-9
- Llombart-Bosch, A., Machado, L., Navarro, S., Bertoni, F., Bacchini, P., Alberghini, M., et al. (2009). Histological heterogeneity of Ewing's sarcoma/PNET: an immunohistochemical analysis of 415 genetically confirmed cases with clinical support. *Virchows Arch.* 455 (5), 397–411. doi:10.1007/s00428-009-0842-7
- Patrizi, S., Miele, E., Falcone, L., Vallese, S., Rossi, S., Barresi, S., et al. (2024). Malignant peripheral nerve sheath tumor (MPNST) and MPNST-like entities are defined by a specific DNA methylation profile in pediatric and juvenile population. *Clin. Epigenetics* 16, 9. doi:10.1186/s13148-023-01621-7
- Paydas, S., Bagir, E. K., Deveci, M. A., and Gonlusen, G. (2016). Clinical and prognostic significance of PD-1 and PD-L1 expression in sarcomas. *Med. Oncol.* 33 (8), 93. doi:10.1007/s12032-016-0807-z
- Pfister, S. M., Reyes-Múgica, M., Chan, J. K. C., Hasle, H., Lazar, A. J., Rossi, S., et al. (2022). A summary of the inaugural WHO classification of pediatric tumors: transitioning from the optical into the molecular era. *Cancer Discov.* 12 (2), 331–355. doi:10.1158/2159-8290.cd-21-1094
- Robinson, E. L., Baker, A. H., Brittan, M., McCracken, I., Condorelli, G., Emanuelli, C., et al. (2022). Dissecting the transcriptome in cardiovascular disease. *Cardiovasc. Res.* 118 (4), 1004–1019. doi:10.1093/cvr/cvab117
- Salgado, C. M., Alaggio, R., Ciolfi, A., Zin, A., Diomedei Camassei, F., Pedace, L., et al. (2023). Pediatric BCOR-altered tumors from soft tissue/kidney display specific DNA methylation profiles. *Mod. Pathol.* 36 (2), 100039. doi:10.1016/j.modpat.2022.100039
- Sbaraglia, M., Bellan, E., and Tos, A. P. D. (2021). The 2020 WHO classification of soft tissue tumours: news and perspectives. *Pathol. - J. Ital. Soc. Anat. Pathol. Diagn. Cytopathol.* 113, 70–84. doi:10.32074/1591-951X-213
- Sorensen, P. H., and Triche, T. J. (1996). Gene fusions encoding chimaeric transcription factors in solid tumours. *Semin. Cancer Biol.* 7 (1), 3–14. doi:10.1006/scbi.1996.0002
- Stahl, D., Gentles, A. J., Thiele, R., and Gütgemann, I. (2019). Prognostic profiling of the immune cell microenvironment in Ewing's Sarcoma Family of Tumors. *Oncimmunology* 8 (12), e1674113. doi:10.1080/2162402x.2019.1674113
- Stranger, B. E., Forrest, M. S., Dunning, M., Ingle, C. E., Beazley, C., Thorne, N., et al. (2007). Relative impact of nucleotide and copy number variation on gene expression phenotypes. *Science* 315 (5813), 848–853. doi:10.1126/science.1136678
- Teschendorff, A. E., Marabita, F., Lechner, M., Bartlett, T., Tegner, J., Gomez-Cabrero, D., et al. (2013). A beta-mixture quantile normalization method for correcting probe design bias in Illumina Infinium 450 k DNA methylation data. *Bioinformatics* 29 (2), 189–196. doi:10.1093/bioinformatics/bts680
- Tian, Y., Morris, T. J., Webster, A. P., Yang, Z., Beck, S., Feber, A., et al. (2017). ChAMP: updated methylation analysis pipeline for Illumina BeadChips. *Bioinformatics* 33 (24), 3982–3984. doi:10.1093/bioinformatics/btx513
- Visser, L. L., Bleijs, M., Margaritis, T., van de Wetering, M., Holstege, F. C. P., and Clevers, H. (2023). Ewing sarcoma single-cell transcriptome analysis reveals functionally impaired antigen-presenting cells. *Cancer Res. Commun.* 3 (10), 2158–2169. doi:10.1158/2767-9764.crc-23-0027
- Wang, L., Geng, H., Liu, Y., Liu, L., Chen, Y., Wu, F., et al. (2023). Hot and cold tumors: immunological features and the therapeutic strategies. *MedComm* 4 (5), e343. doi:10.1002/mco.2343
- Weeden, C. E., Gayevskiy, V., Marceaux, C., Batey, D., Tan, T., Yokote, K., et al. (2023). Early immune pressure initiated by tissue-resident memory T cells sculpts tumor evolution in non-small cell lung cancer. *Cancer Cell* 41 (5), 837–852.e6. doi:10.1016/j.ccell.2023.03.019
- Yoshida, A. (2023). Ewing and Ewing-like sarcomas: a morphological guide through genetically-defined entities. *Pathol. Int.* 73 (1), 12–26. doi:10.1111/pin.13293